

Supplementary Figures 1 to 14

Concurrent Activation of Striatal Direct and Indirect Pathways During Action Initiation

Guohong Cui^{1*}, Sang Beom Jun^{5*}, Xin Jin^{1,6}, Michael D. Pham¹, Steven S. Vogel^{3#}, David M. Lovinger^{1,2#} & Rui M. Costa^{1,4,#}

¹Section on In Vivo Neural Function, ²Section on Synaptic Pharmacology, Laboratory for Integrative Neuroscience, ³Section on Cellular Biophotonics, Laboratory for Molecular Physiology, NIAAA, NIH, Bethesda, MD, USA

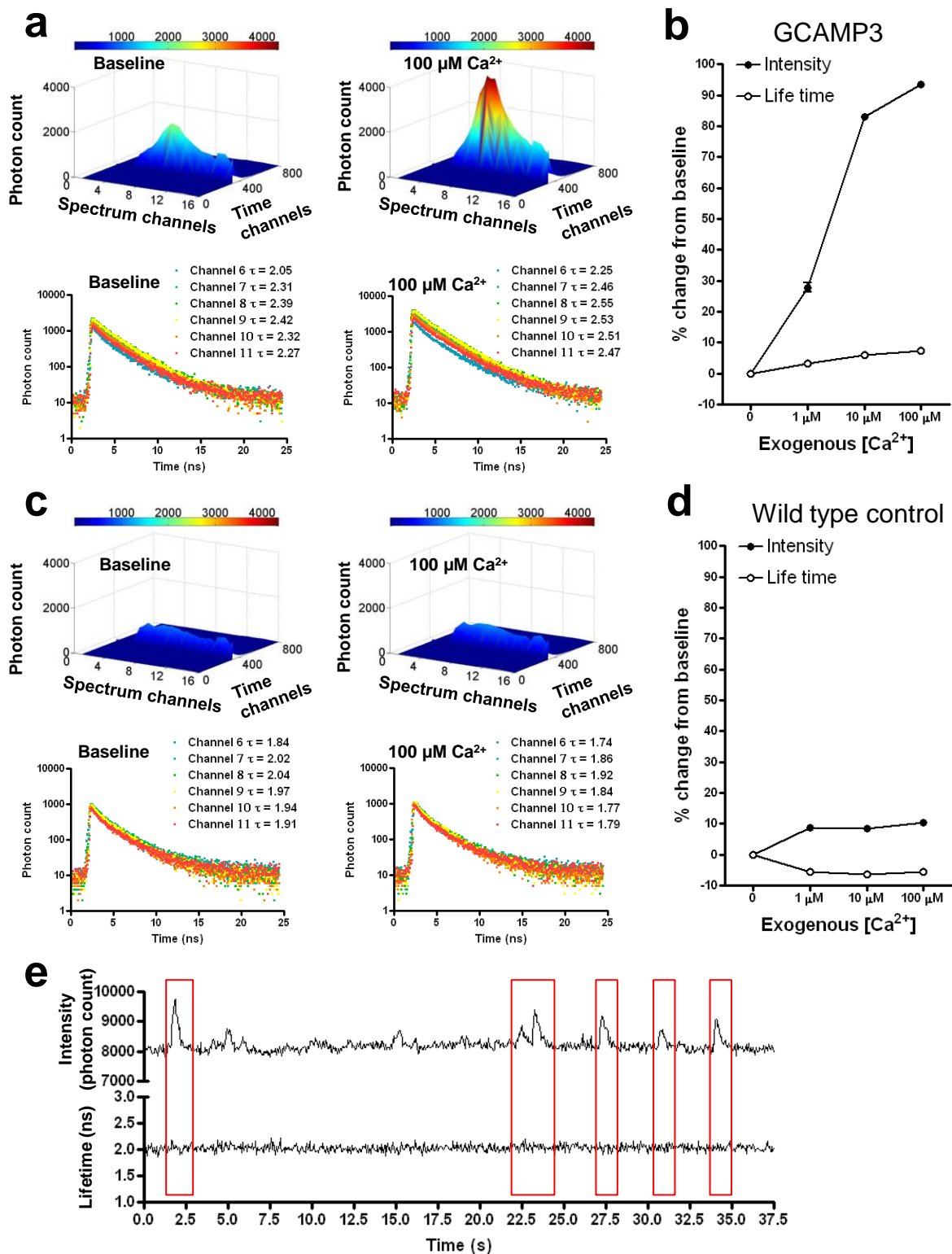
⁴ Champalimaud Neuroscience Programme at Instituto Gulbenkian de Ciência and Champalimaud Centre for the Unknown, Lisbon, Portugal

⁵Department of Electronics Engineering, Ewha Womans University, Seoul, Korea

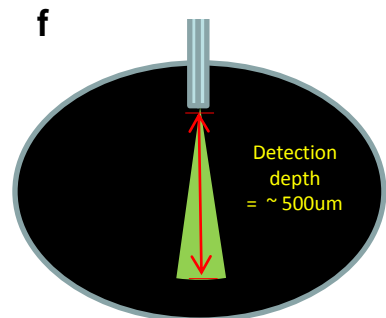
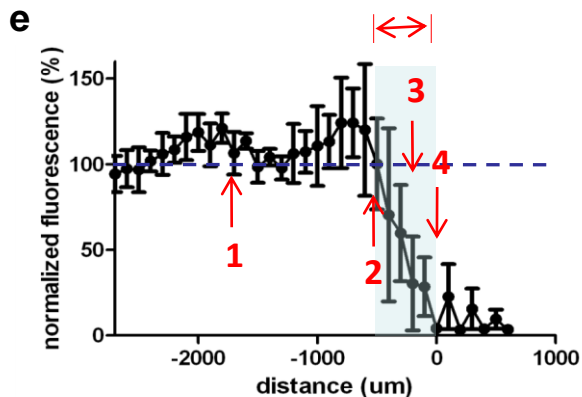
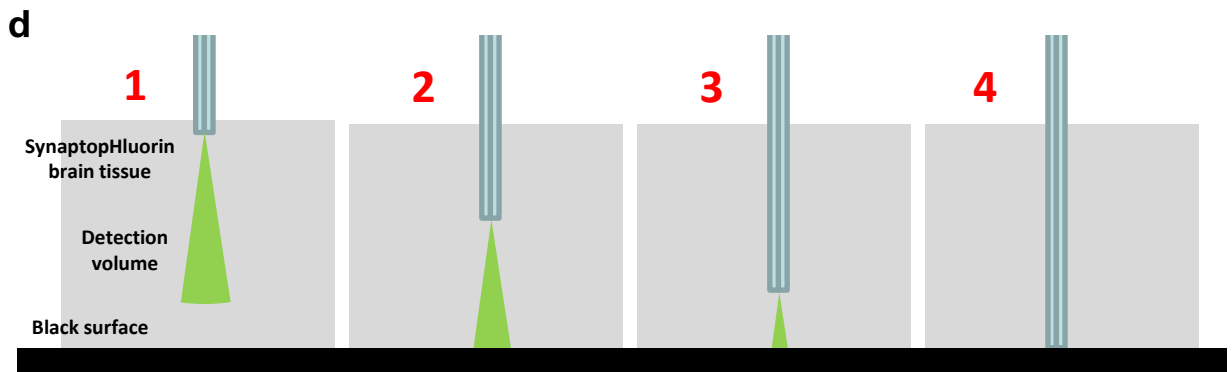
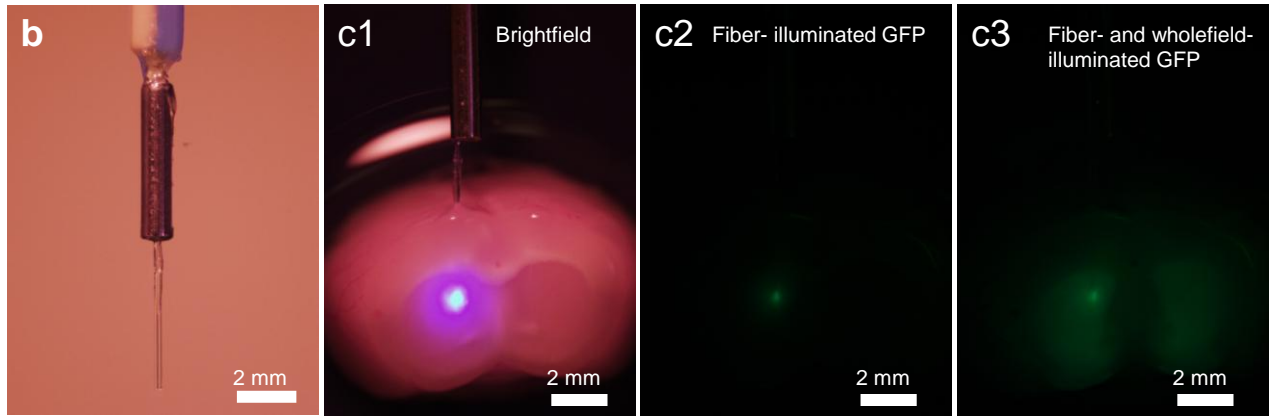
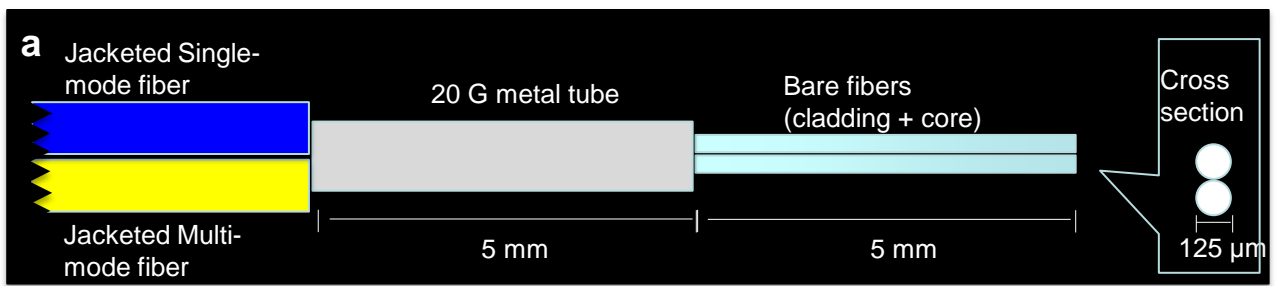
⁶ Molecular Neurobiology Laboratory, The Salk Institute for Biological Studies, 10010 North Torrey Pines Road, La Jolla, California 92037, USA

* Equal contributions to this study.

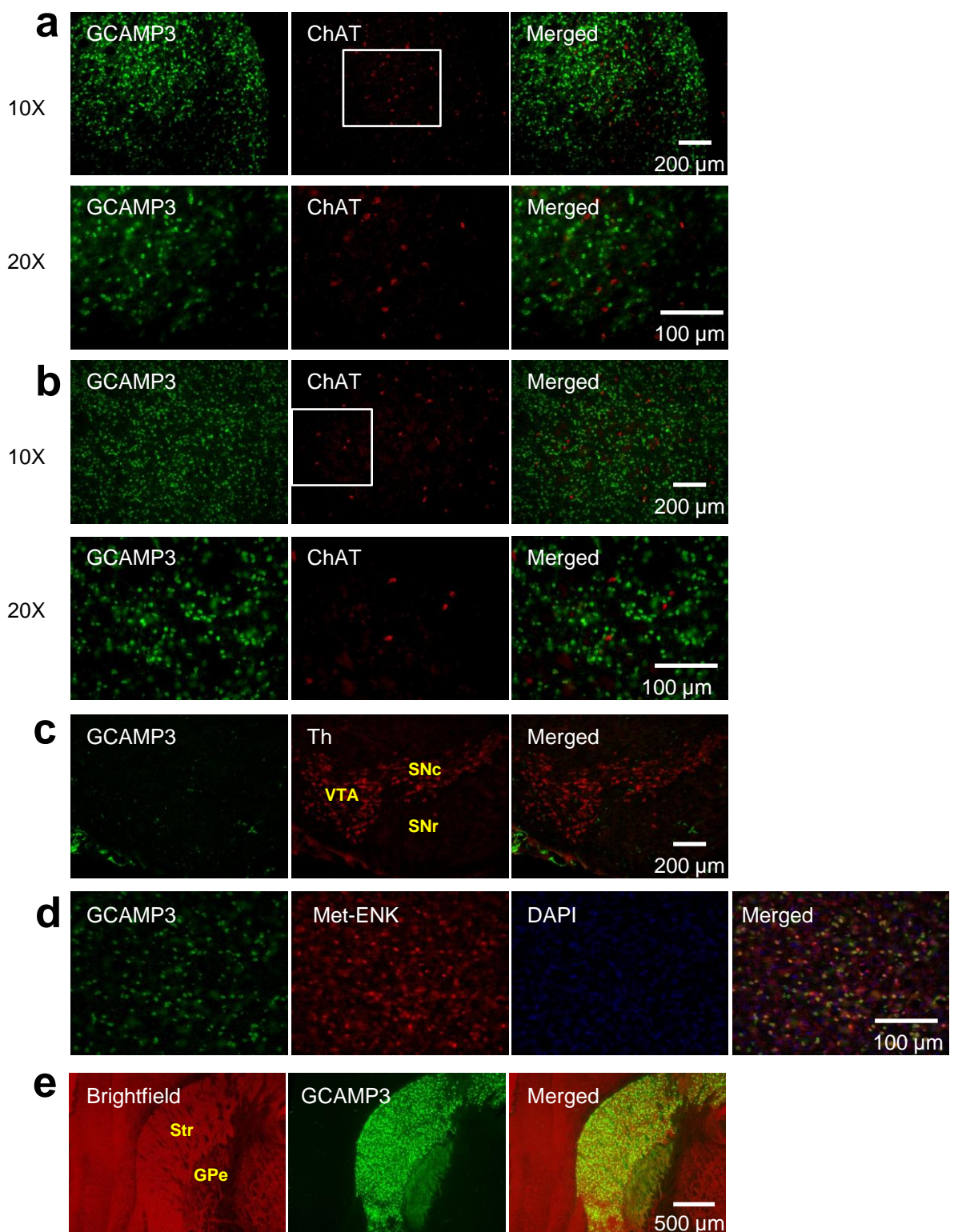
Corresponding author



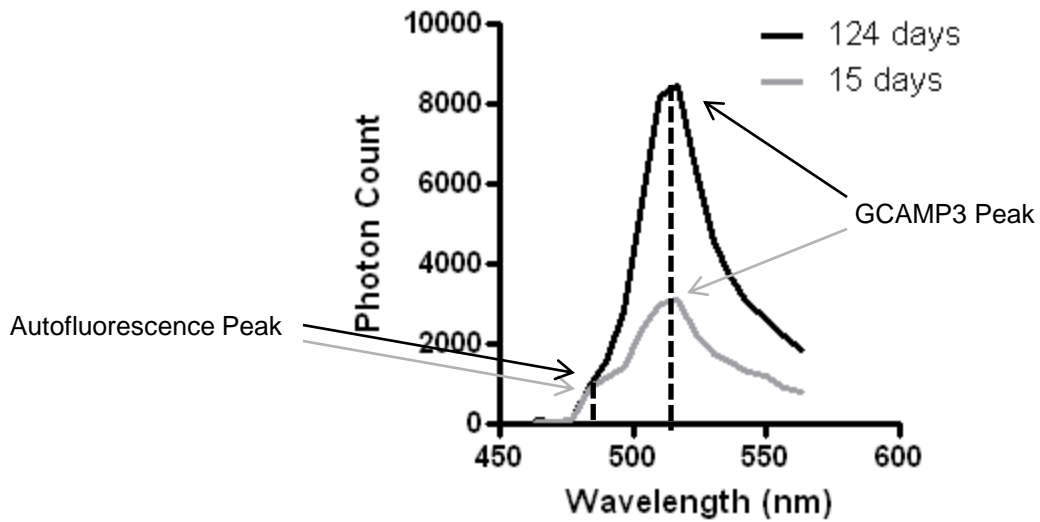
Supplementary Figure 1. The fluorescence lifetime of GCAMP3 does not show significant Ca^{2+} -dependent changes in vitro or in vivo. **a-d**, In vitro measurement of fluorescence intensity and lifetime in the supernatant of homogenized striatal tissue from an AAV Flex-GCAMP3 injected A2A-Cre mouse (**a,b**) and non-injected A2A-Cre mouse (**c,d**). Top panels in **a, c** are GCAMP3 (**a**) and autofluorescence (**c**) spectra captured at the baseline (no exogenous Ca^{2+}) and in $100 \mu\text{M} \text{Ca}^{2+}$. Bottom panels in **a, c** are GCAMP3 fluorescence (**a**) and autofluorescence (**c**) lifetime decay curve and calculated lifetime constant captured at the baseline (no exogenous Ca^{2+}) and in $100 \mu\text{M} \text{Ca}^{2+}$. **b, d**, Comparison of the % change in the intensity and lifetime of GCAMP3 (**b**) and autofluorescence (**d**) with various concentrations of Ca^{2+} . **e**, Fluorescence intensity (top) and corresponding lifetime (bottom) recorded in a freely moving AAV Flex-GCAMP3 injected A2A-Cre mouse. Boxed areas are to highlight that there were no detectable lifetime changes even when there were large increases in the intensity.



Supplementary Figure 2. Estimating the detection range of a hybrid fiber probe. **a, b**, illustration (**a**) and actual picture (**b**) of a hybrid fiber probe. **c1-c3**, Estimating the volume of fluorescent brain tissue (from D2-GFP mice) that can be excited by laser emitted from the fiber. **c1**, Brightfield photo to show the general structure of fiber and brain tissue. **c2**, 473 nm laser from fiber tip excites GFP-expressing tissue for extending to a depth of $\sim 500\mu\text{m}$ from the probe tip. **c3**, whole-field illumination was added to show the total excitable GFP tissue. **d, e**, Schematic diagram of the experimental procedures (**d**) and results (**e**) of the experiment estimating the detection depth in fluorescent brain tissue using TCSPC system. See Supplementary Methods for full description. **f**, Schematic summary to show the detection depth of the system using hybrid probe is approximately $500\mu\text{m}$ in the brain.



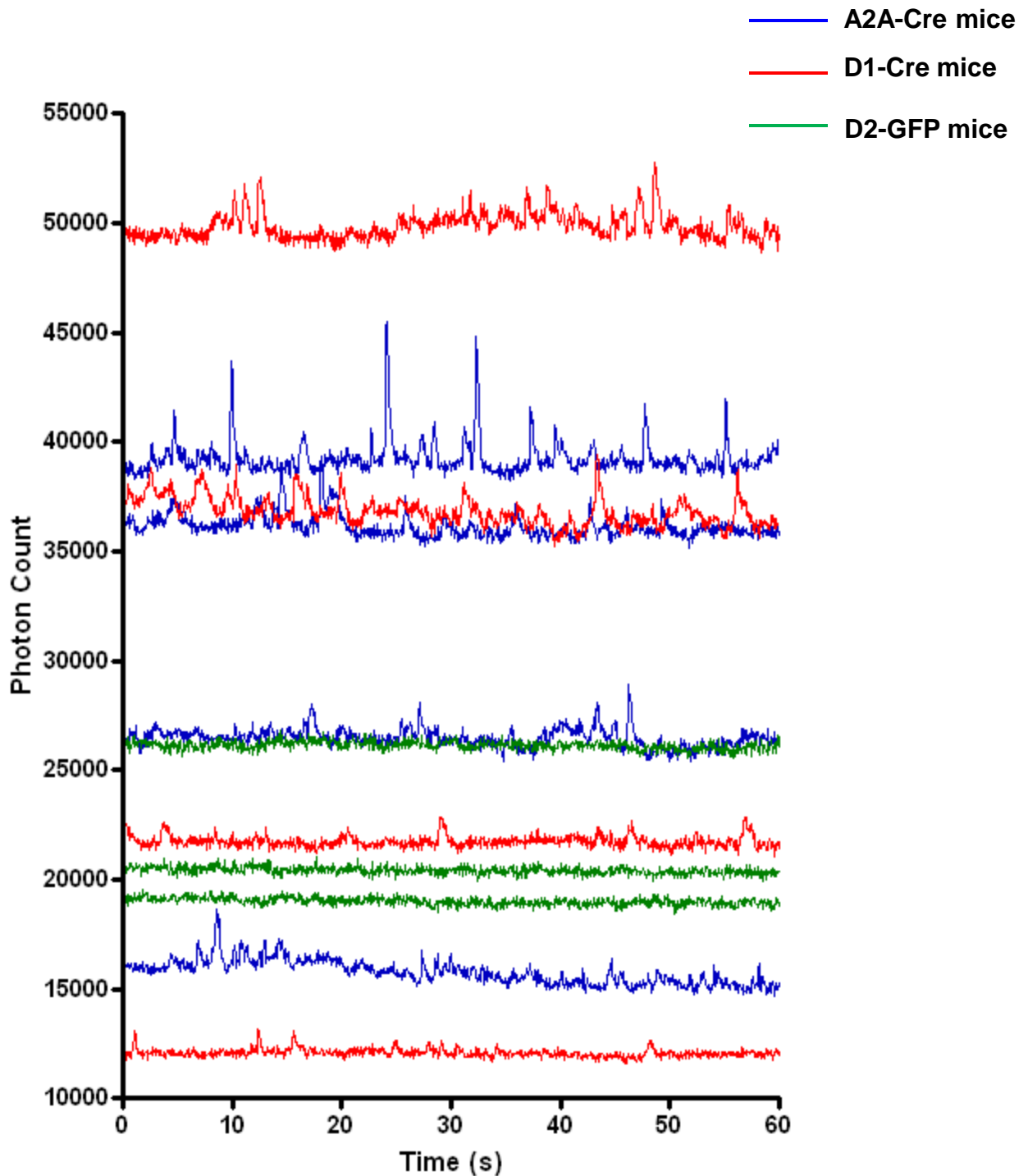
Supplementary Figure 3. GCAMP3 is specifically expressed in indirect-pathway SPNs in A2A-Cre mice via either viral expression or by crossing with GCAMP3 reporter mice. **a, b**, Double immuno-labeling for GCAMP3 and ChAT (specific marker for cholinergic interneurons) in AAV Flex-GCAMP3 injected A2A-Cre mice (**a**) and A2A-Cre;Flox-stop-GCAMP3 double mutant mice (**b**). Note there is no co-localization of ChAT and GCAMP3. **c**, Double immuno-staining for GCAMP3 and tyrosine hydroxylase (TH) (specific marker for catecholamine-producing neurons) to show GCAMP3 is not expressed in midbrain dopaminergic neurons, nor in the terminal field (SNr) of direct-pathway SPNs in A2A-Cre;Flox-stop-GCAMP3 double mutant mice. **d**, Triple-labeling for GCAMP3, Met-enkephalin (specific marker for indirect-pathway SPNs) and nucleus (DAPI staining) in A2A-Cre;Flox-stop-GCAMP3 double mutant mice to show GCAMP3 is specifically in indirect-pathway SPNs. **e**, Images of bright-field and GCAMP3 immuno-staining to show the soma (in the striatum) and terminal (GPe) fields of indirect-pathway SPNs.



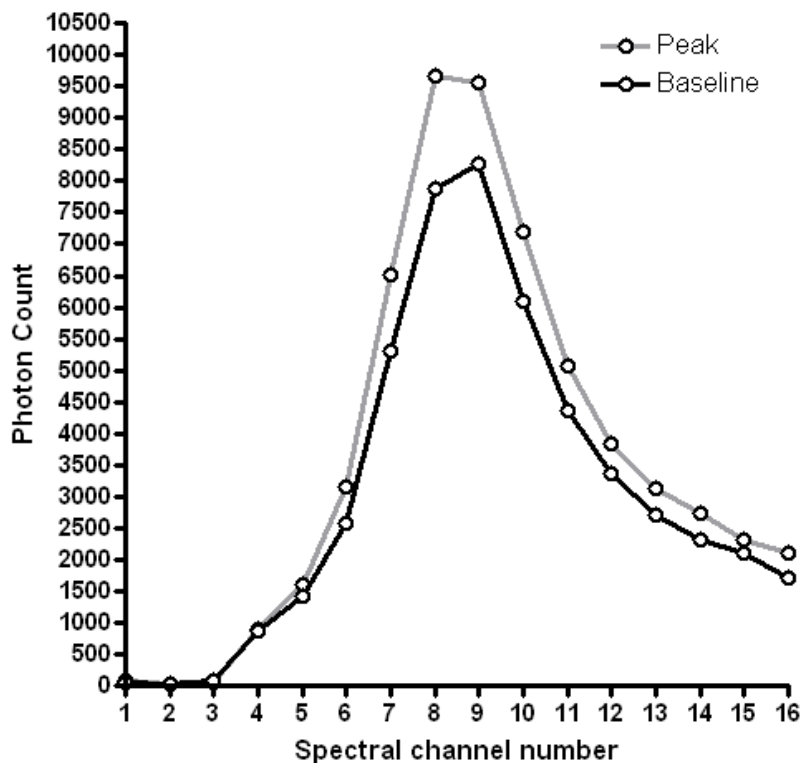
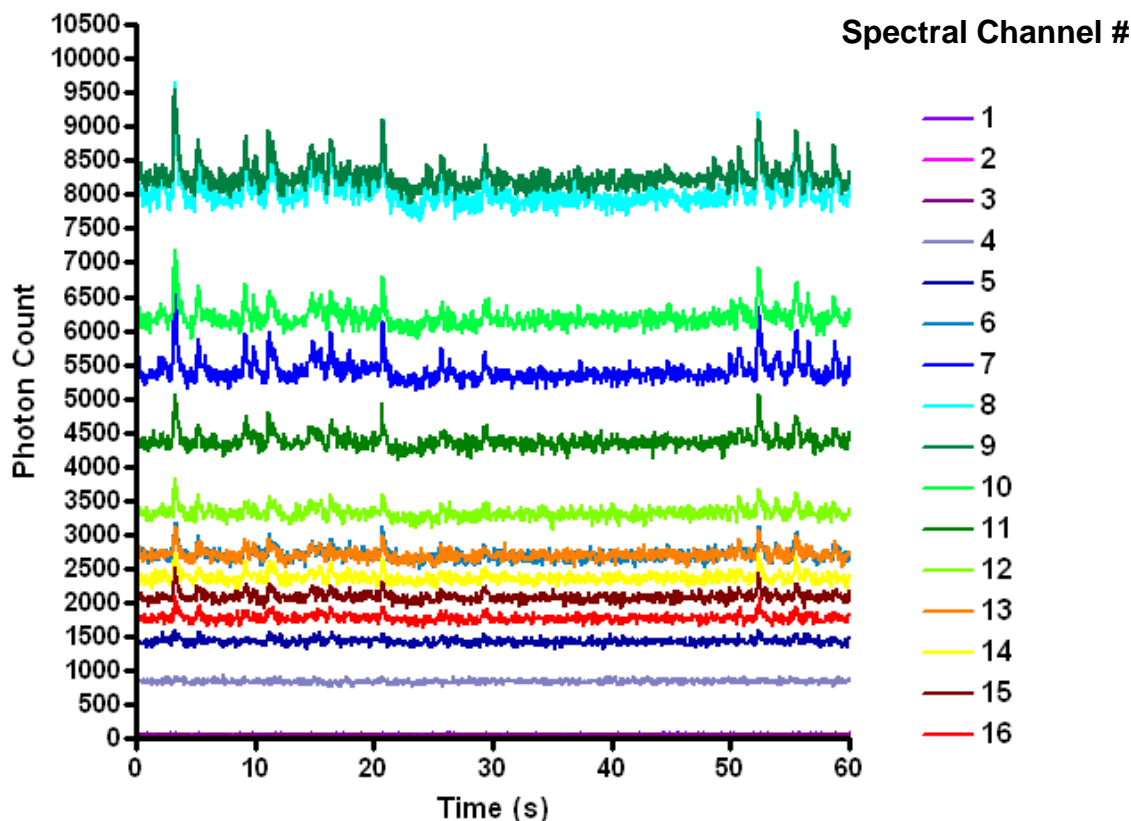
15 days: $\text{Peak}_{\text{GCAMP3}} / \text{Peak}_{\text{Autofluorescence}}$ Ratio = 3.4

124 days: $\text{Peak}_{\text{GCAMP3}} / \text{Peak}_{\text{Autofluorescence}}$ Ratio = 8.8

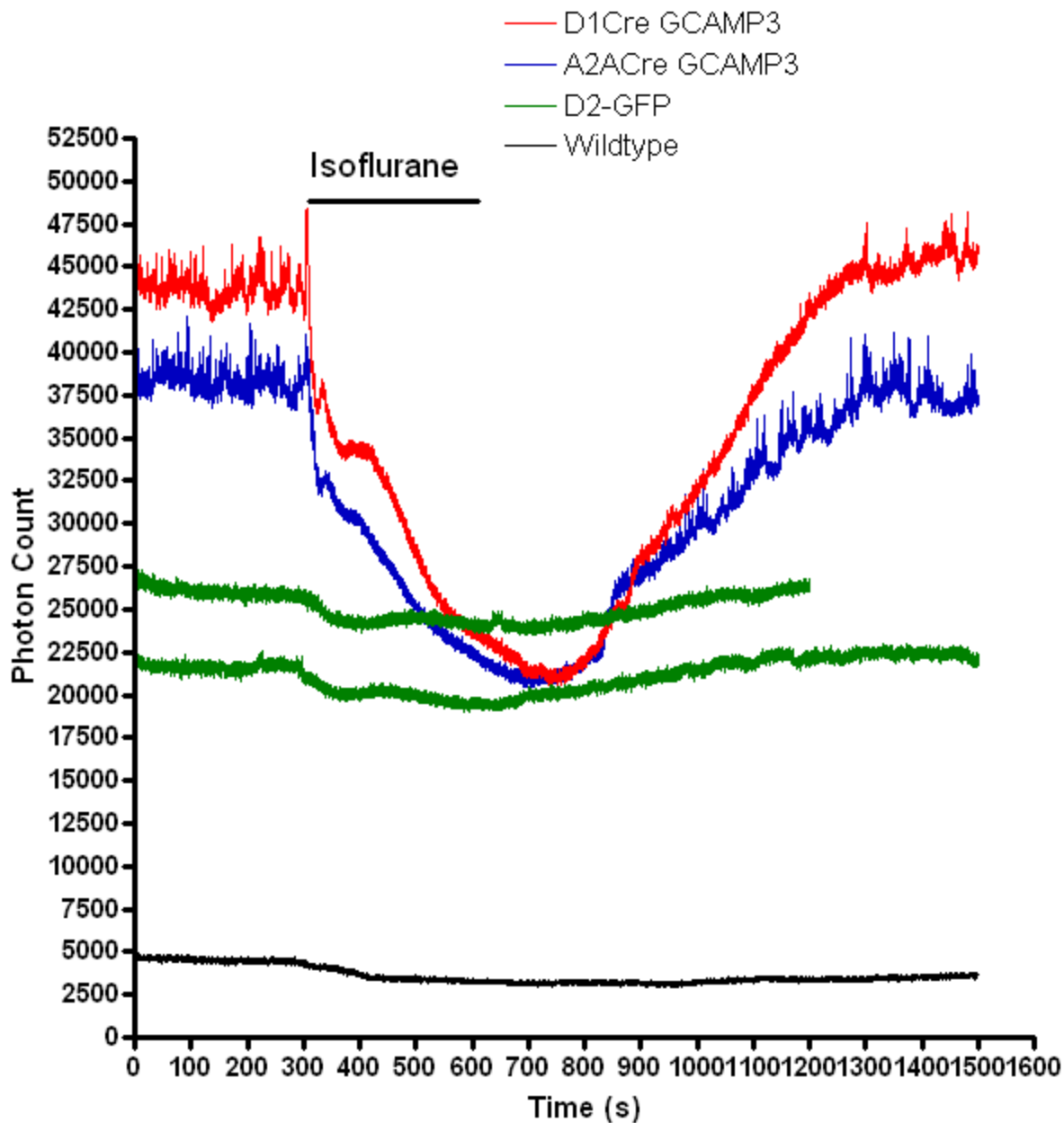
Supplementary Figure 4. Comparison of GCAMP3 spectrum at two weeks and 4 months after virus injection. The two GCAMP3 fluorescence spectra were measured from the same site in the same animal (A2A-Cre mouse) at 15 days and 124 days after AAV-FIEx-GCAMP3 injection.



Supplementary Figure 5. Absolute GCAMP3 fluorescence intensity in freely moving animals. Example traces showing absolute fluorescence intensity (calculated by summation of photon counts from 8 peak spectral channels) recorded over 1 min from 4 AAV-injected A2A-Cre mice (blue traces), 4 AAV-injected D1-Cre mice (red traces) and 3 D2GFP control mice (green traces).

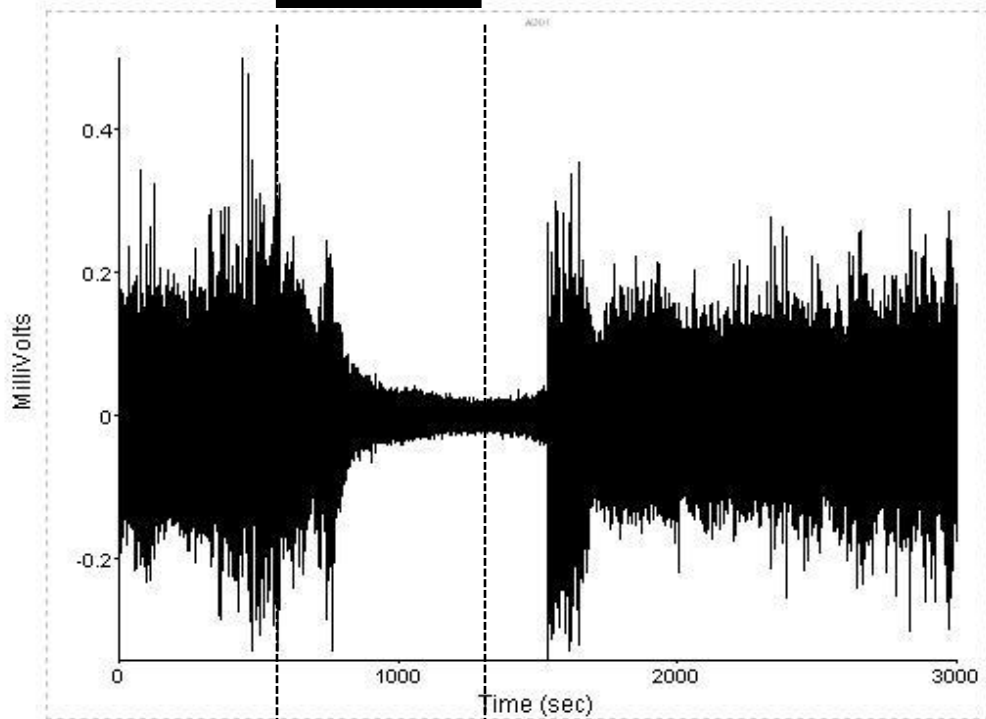
a**b**

Supplementary Figure 6. Multichannel fluorescence responses in a freely moving AAV Flex-GCAMP3 injected A2A-Cre mouse. a, GCAMP3 spectrum captured at the baseline (time 1.05 s in **b**) and at the peak of a fluorescence transient (time 3.25 s in **b**). **b,** Time-lapsed fluorescence changes of individual spectral channels recorded over 60 s. Integrated photon counts of peak GCAMP3 spectral channels (channel 6-13) were used to calculate the fluorescence intensity of GCAMP3 throughout this study.

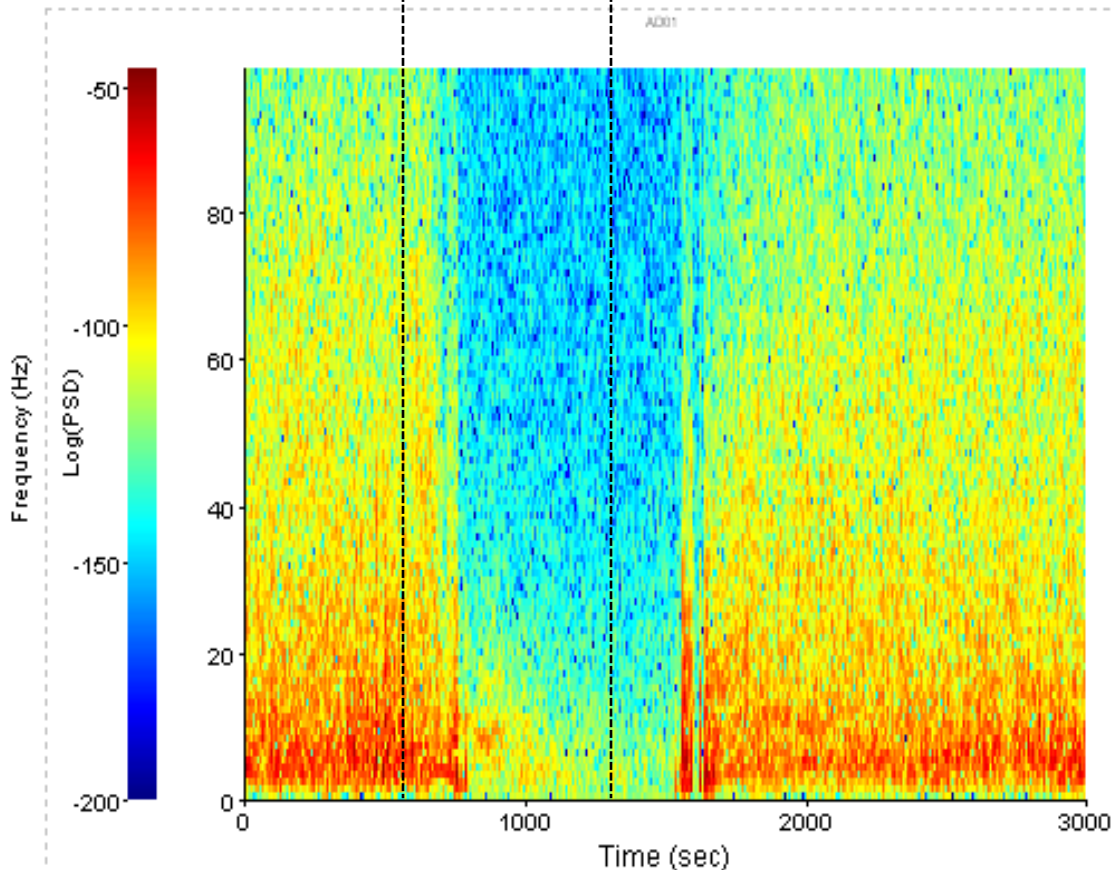


Supplementary Figure 7. Effect of isoflurane anesthesia on GCAMP3 fluorescence, D2-GFP and autofluorescence. GCAMP3 fluorescence transients were abolished by isoflurane. A small decrease in baseline fluorescence was also observed in D2-GFP mice and non-fluorescent wildtype mice, suggesting that part of the isoflurane-induced baseline drop in GCAMP3 fluorescence involved non-neuronal activity dependent mechanisms. Thus, we focused on the GCAMP3 transients as a measurement of neuronal activity in this study.

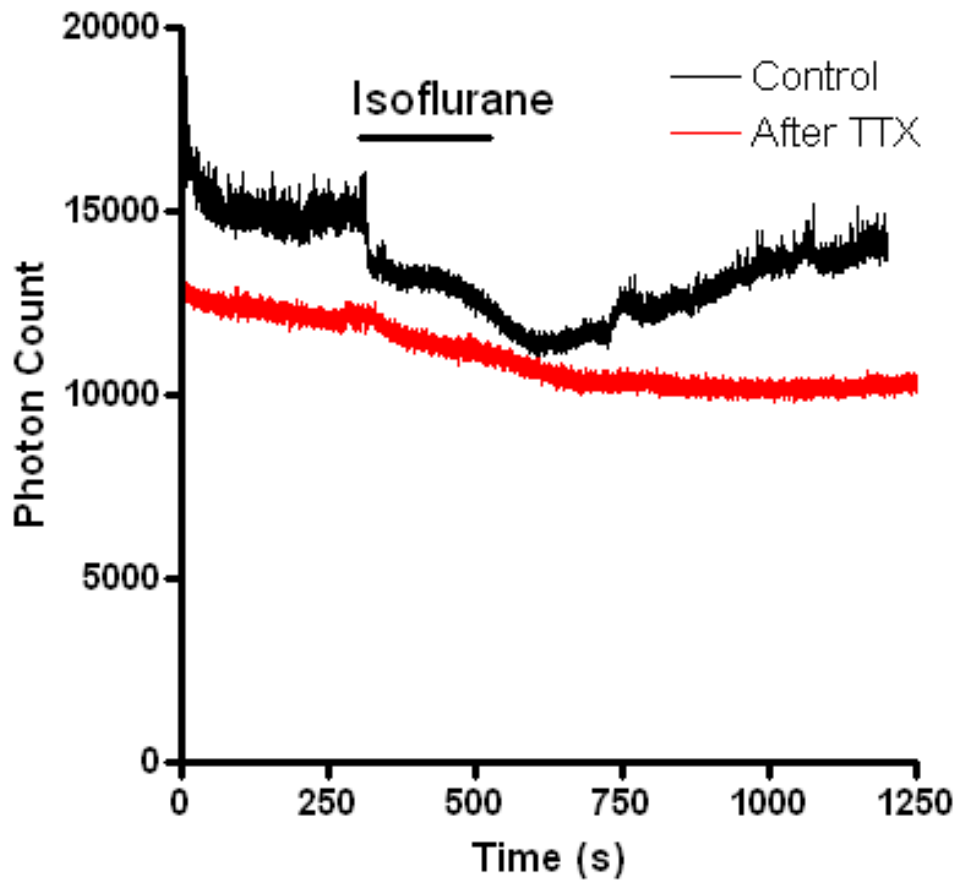
Isoflurane



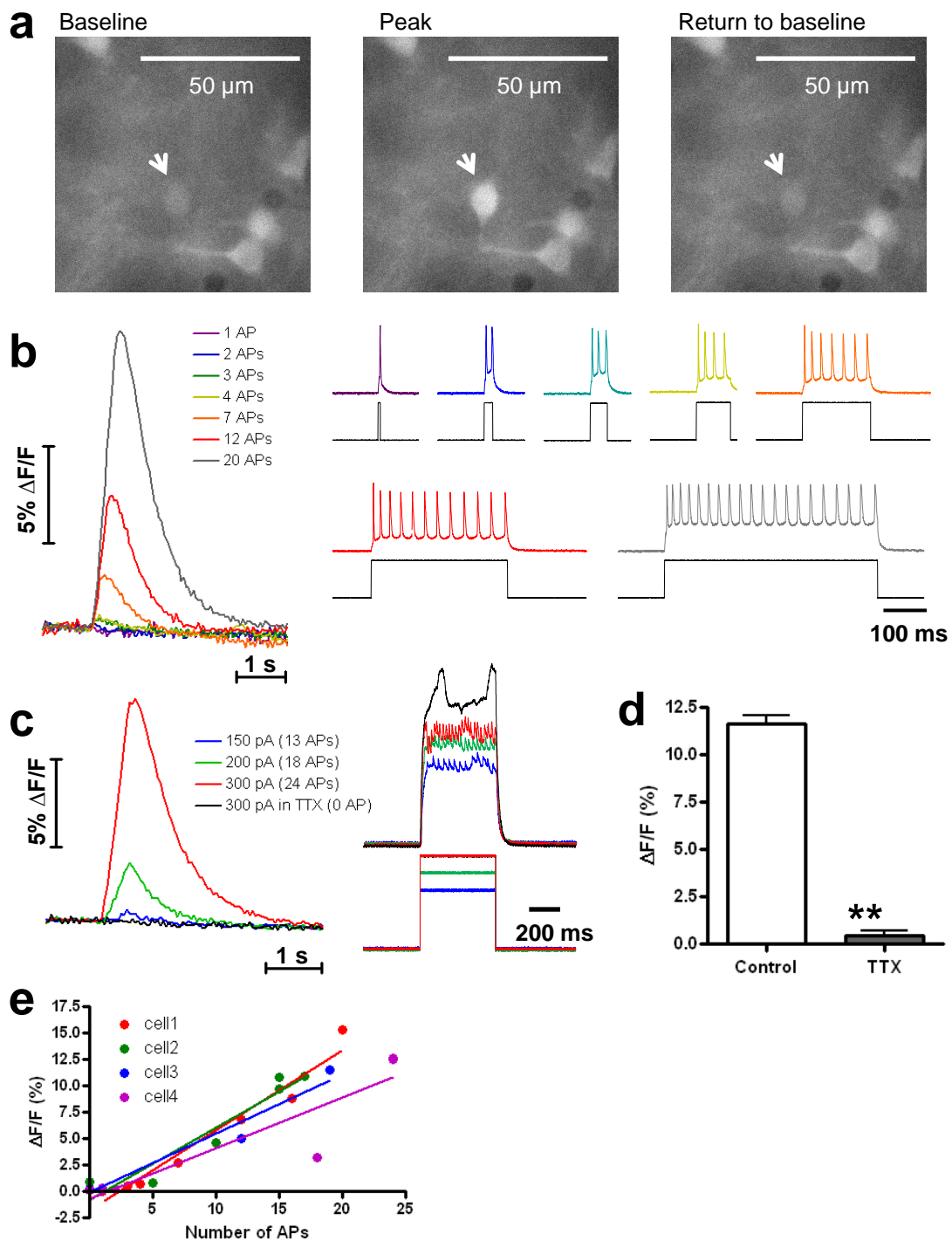
Spectrogram Analysis



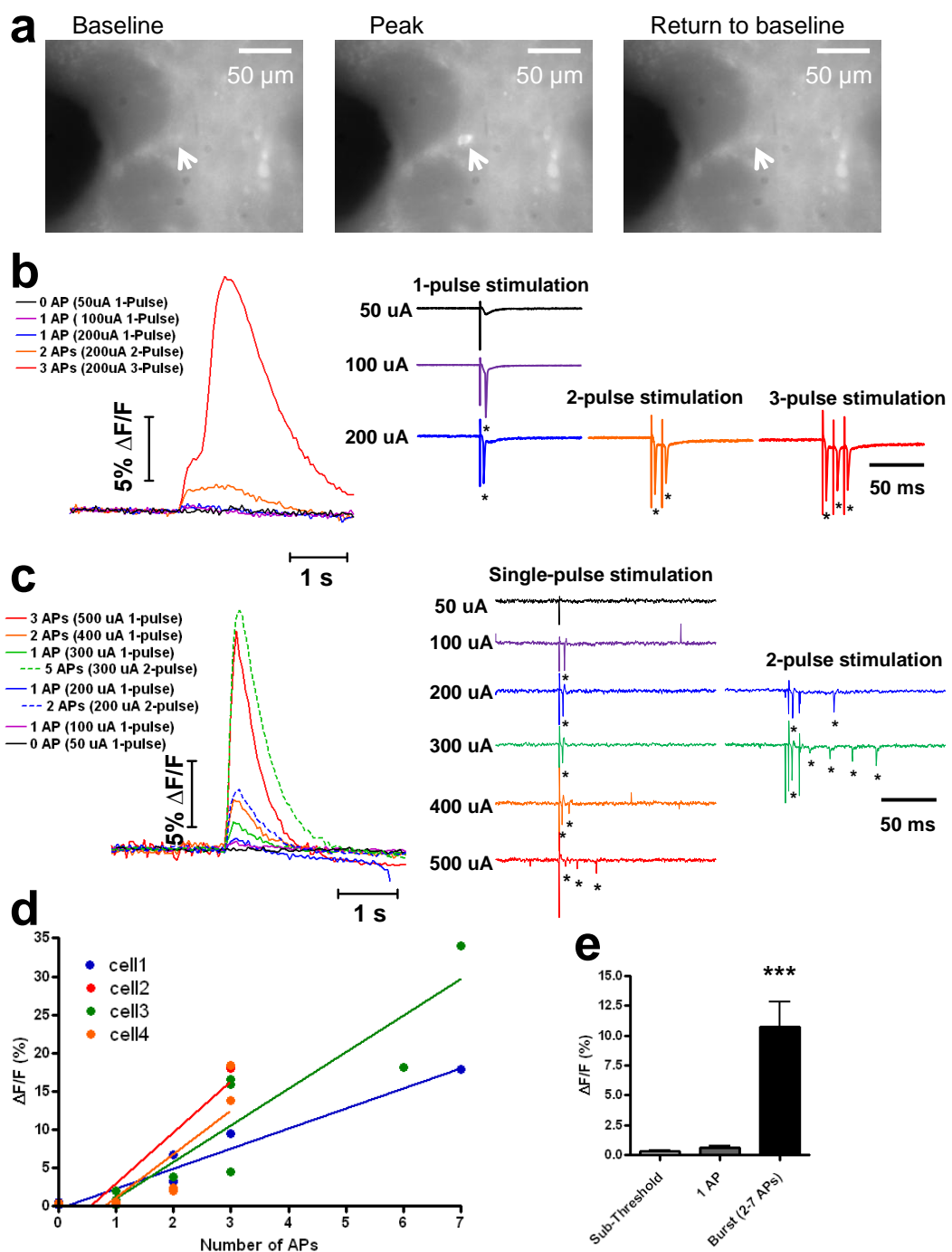
Supplementary Figure 8. Isoflurane anesthesia abolished the local neural activity in the striatum. The amplitude (top) and the power density spectrum (PSD) of local field potential (LFP) in the striatum were both reversibly affected by isoflurane.



Supplementary Figure 9. In vivo GCAMP3 transients diminish after intra-striatal TTX infusion. The effect of isoflurane is occluded by previous TTX application, indicating that both TTX and isoflurane can block GCAMP3 transients.

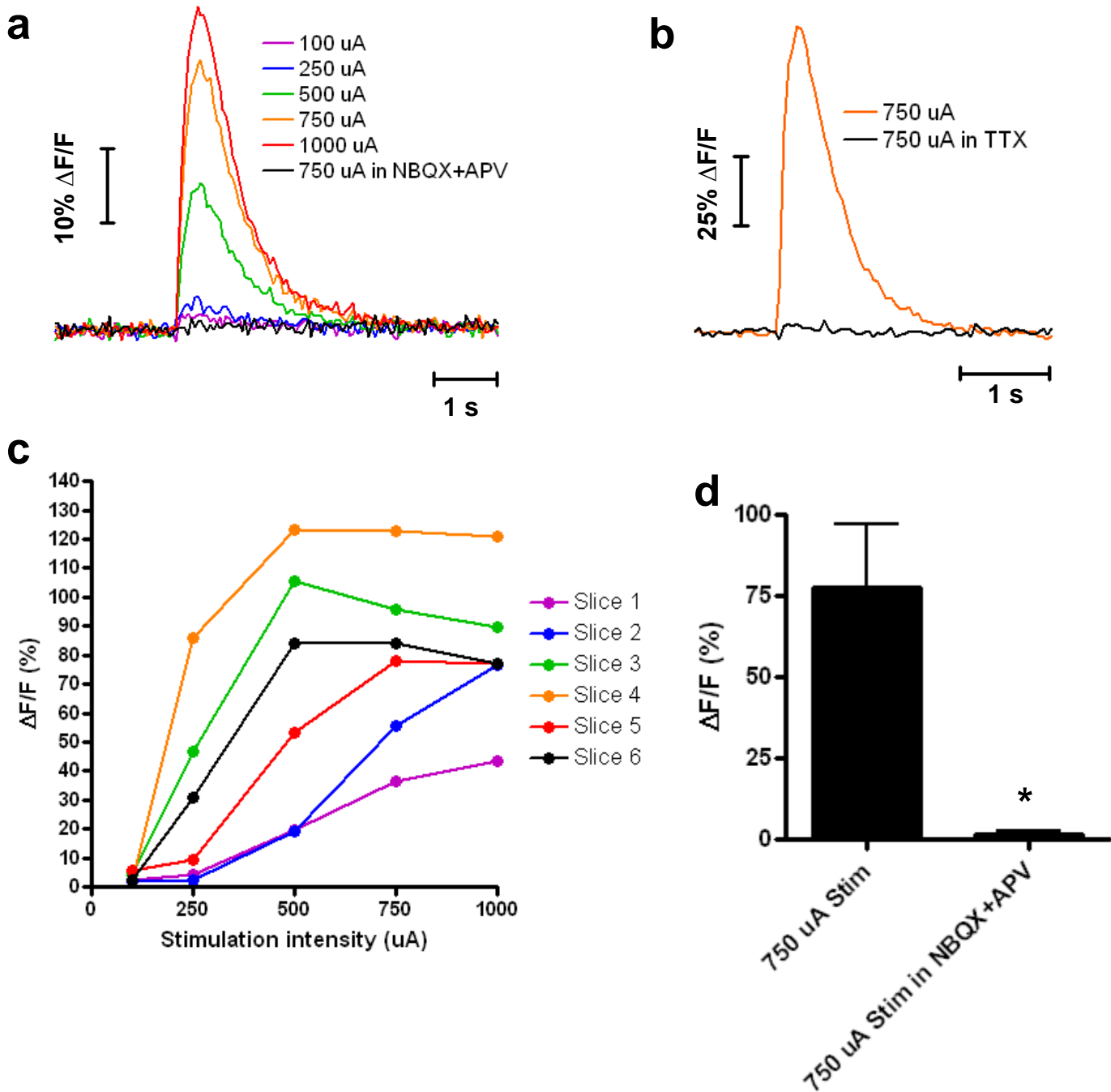


Supplementary Figure 10. GCAMP3 fluorescence reports bursts of action potentials evoked by current injection in acute striatal slices. **a**, Fluorescence images of a GCAMP3-expressing SPN (white arrow) taken before, during and after a burst of action potentials (20 APs) evoked by current injection (a 400 pA, 487.5ms square pulse) through a patch pipette. See supplementary movie 2 for full series of time-lapsed images. **b**, Single-trial traces of GCAMP3 fluorescence changes (left) in response to different numbers of APs (right) evoked by a 400 pA current pulse of various durations (from top left to bottom right: 4.88, 19.5, 39, 78, 156, 312, 487.5 ms). The fluorescence imaging and simultaneous cell-attached recording was performed on the SPN shown in (a). **c**, Traces of simultaneous fluorescence imaging (left) and cell-attached firing recording (right) from another GCAMP3-expressing SPN to show the relationship between the GCAMP3 fluorescence change and the number of action potentials evoked by a 487.5 ms current pulse of various current intensities. Note TTX (1 μM) blocked both APs and the fluorescence transient evoked by the 300 pA current injection, suggesting that GCAMP3 fluorescence change was dependent on evoked APs but not on the current pulse per se. **d**, Summary of TTX (1 μM) effect on GCAMP3 fluorescence evoked by current injection (300 pA, 487.5 ms) from 3 cells. ** $p < 0.01$, paired t-test. **e**, Summary of the relationship between GCAMP3 fluorescence and the number of current injection-evoked APs from 4 cells.

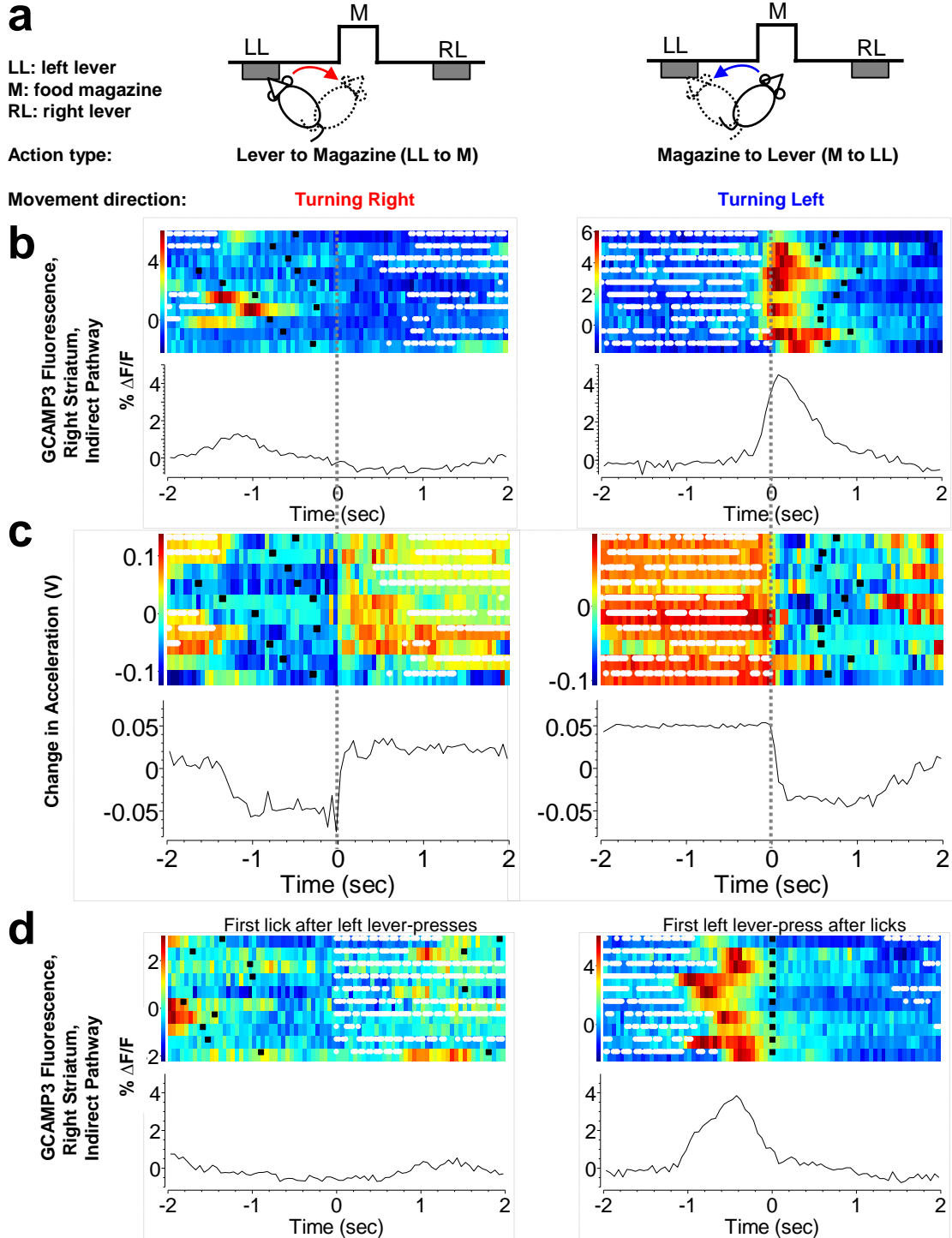


Supplementary Figure 11. GCAMP3 fluorescence reports bursts of action potentials evoked by synaptic stimulation in acute brain slices. **a**, Fluorescence images of a GCAMP3-expressing SPN (white arrow) taken before, during and after a burst of action potentials (3 APs) evoked by local synaptic stimulation (a 200 uA, 0.2 ms train 3 stimulations at 100 Hz). The tip of the stimulating electrode is seen on the left edge of the image (black round shade). See supplementary movie 3 for full series of time-lapsed images. **b**, Single-trial traces of GCAMP3 fluorescence changes (left) and the corresponding currents (right) evoked by different synaptic stimulation parameters. * indicates evoked “action current” recorded with cell-attached voltage-clamp recording. The fluorescence imaging and simultaneous cell-attached recording was performed on the SPN shown in (**a**). **c**,

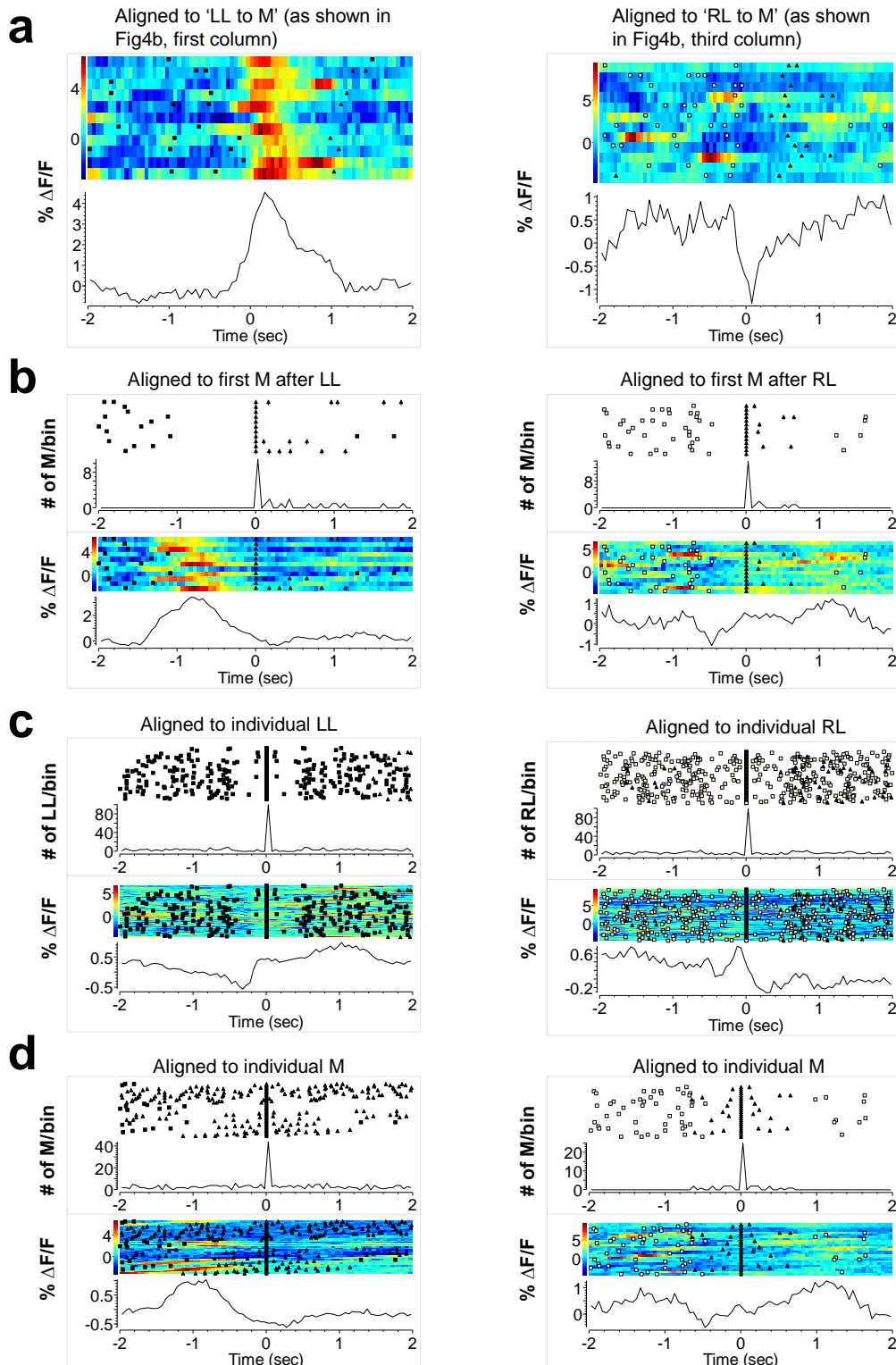
Traces of simultaneous fluorescence imaging (left) and cell-attached firing recording (right) from another GCAMP3-expressing SPN to show the relationship between the GCAMP3 fluorescence change and the number of action potentials evoked by 0.2 ms single-pulse stimulation at increasing intensities (from 50 μ A to 500 μ A). 2-pulse (at 100 Hz) stimulations at 200 and 300 were also performed on this cell for comparison. **d**, Summary of the relationship between GCAMP3 fluorescence and the number of synaptic driven APs from 4 cells. **e**, Comparison of the GCAMP3 fluorescence changes between subthreshold synaptic stimulation, synaptically- driven single AP, and the synaptically driven burst of APs with physiologically relevant number of spikes. ** $p < 0.001$, one-ANOVA followed by Bonferroni's Multiple Comparison Test (burst vs single AP and burst vs subthreshold).



Supplementary Figure 12. Optical measurement of populational neuronal activity of SPNs evoked by synaptic stimulation in acute brain slices of A2A-Cre;flox-stop GCAMP3 reporter mice. To relate GCAMP3 fluorescence imaging results acquired by sCMOS camera to our in vivo fluorescence data measured by TSPCS-based optical fiber probes, we used the same synaptic stimulation method to evoke neuronal responses in acute brain slices and measured GCAMP3 fluorescence using our in vivo optical fiber system. **a**, Traces of GCAMP3 fluorescence responses evoked by single-pulse synaptic stimulation of various intensities (100 μA to 1000 μA). Ionotropic glutamate receptor blockers (50 μM APV + 5 μM NBQX) completely blocked the fluorescence response evoked by 750 μA stimulation. **b**, Example traces of GCAMP3 fluorescence evoked by 750 μA synaptic stimulation before and after TTX (1 μM) application. **c**, Summary of the relationship between GCAMP3 fluorescence and the single-pulse stimulation intensity from 6 brain slices of 3 animals. **d**, Comparison of the GCAMP3 fluorescence changes evoked by 750 μA stimulation before and after APV (50 μM and NBQX (5 μM) application. * $p=0.029$, paired t-test, $n=4$.



Supplementary Figure 13. Right striatum activation precedes leftward turning behavior. To complement the results shown in Figure 4, which were recorded in the left striatum, we measured GCAMP3 fluorescence from the right dorsal striatum of an A2A-Cre mouse injected with AAV FLEX-GCAMP3. To monitor the head movement with higher temporal resolution and sensitivity, we attached a 3-axis acceleromter (ADXL 335) to the head of the mouse. Changes in the acceleration in each axis are represented by changes in the output voltage. **a**, Illustration of 2 types of actions in a left-lever FR10 operant task that were analyzed. Sucrose solution (20%) was used as the reward. Left panel: initiation of rightward movement from left lever (LL) to food magazine (M). Right panel: initiation of leftward movement from M to LL. Movement initiation was defined as the first frame of movement toward the target direction in video files captured at 30 frames/s. **b**, GCAMP3 fluorescence changes in the indirect-pathway SPNs measured in the right striatum, aligned to the initiation of the corresponding actions illustrated in (**a**). Top: 10 trials of color-coded GCAMP3 fluorescence. Bottom: averaged response. **c**, Corresponding changes in the acceleration of the mouse head in trials shown in (**b**). The black squares and white circles in (**b**) and (**c**) are time stamps for left lever presses and licks, respectively. **d**, For direct comparison with (**b**), the GCAMP3 fluorescence is now aligned to the first lick (left) and the first left lever-press in the same trials shown in (**b**).



Supplementary Figure 14. Comparison of GCAMP3 PETH's aligned to different behavioral events from a single D1-Cre mouse in consecutive left lever and right lever pressing sessions. a, GCAMP3 fluorescence changes measured in the left striatum, aligned to the initiation of movement from the left lever (LL) to the food magazine (M) (left column) and the initiation of movement from the right lever (RL) to M (right column). Top: multiple trials of color-coded GCAMP3 fluorescence. Bottom: averaged response of all trials. Symbols of behavioral events: black squares indicate left lever-presses; white squares indicate right lever-presses; black triangles indicate magazine entries. **b**, The same trials as in (a), but the GCAMP3 fluorescence is now aligned to the first magazine entry (M) after left lever-presses (LL) (left column) and to the first M after right lever-presses (RL). Note: the averaged GCAMP3 response is not as sharp as in (a) due to the shift of alignment events. **c**, GCAMP3 fluorescence aligned to individual left lever-presses (LL) (left column) and to individual right lever-presses (RL) (right column). **d**, GCAMP3 fluorescence aligned to individual magazine entries (M) in the left lever-pressing session (left column) and the right lever-pressing session (right column).